Chapter - V

MAGNETIC PROPERTIES

5.0 Introduction

The most important ferrimagnetic substances are certain double oxides of iron and other metals called ferrites. The choice of a ferrite for a particular application is decided by its data on saturation magnetization (Ms), coercive force (Hc), remanence ratio (Mr/Ms), permeability (μ_i), susceptibility (χ) etc.

Hysteresis studies provides useful information on the parameters like the coercive force, saturation magnetization, and remanence ratio.The hysteresis parameters are highly sensitive to crystal structure, heat treatment, chemical composition, porosity and grain size [1].Curie temperature is the temperature above which the spontaneous magnetization vanishes and it separates the disordered paramagnetic state from the ordered ferrimagnetic state. A.C. susceptibility and hysteresis studies at various temperature could provide an idea whether magnetic sample contain multidomain (MD), single domain (SD) or super-paramagnetic (SP) states.

Satya Murthy et al [2] have studied variation of magnetic moment in Ni-Zn ferrites and showed that this system exhibits Y-K type of magnetic ordering. Influence of the presence of Fe^{2+} ion in nickel-zinc ferrite is studied by Srivastava C. M and Patni M.J. [3]. They explained the variation of magnetization with zinc concentration on the basis of the Yafet-Kittel model of spin-canting on the B-sublattice. Mossbauer and magnetic studies of $Ni_{0.4}Zn_{0.6-x}Li_xFe_{2+x}O_4$ are carried out by Puri et al [4]. They explained the result on the basis of preferential site occupancy of different ions and their magnetic interactions. Lattice parameter variation and magnetization studies

on titanium, Zirconium and tin substituted Ni-Zn ferrites are reported by Das et al [5]. They explained the results on the basis of movement of the substituting ions first to tetrahedral and finally to the octahedral sites of the spinel lattice. Ghatage et al [6] have reported neutron diffraction study of Ti substituted Ni-Zn ferrites. They have shown that this ferrite consists of only multidomain particles. Magnetic behavior of $Ni_{1-x}Ge_xFe_2O_4$ is studied by Pandya and Kulkarni [7]. They have shown that, the existence of two ferrimagnetic oxidation states of iron with valencies three and two, having different ordering temperature. X-ray, infrared and magnetic studies of chromium substituted nickel ferrites are reported by Ghatage et al [8]. They observed multidomain and single domain particles are favored in this ferrite.

5.1 Magentostriction

The phenomenon in which the magnetic materials experience changes in dimensions during magnetization is called magnetostriction. This phenomenon was first observed by Joule in 1942. The phenomenon of magnetostriction occupies an important place in relation to both the study of the nature of magnetism and various applications. The coercive force and initial permeability of ferrimagnetic material strongly depends on saturation magnetostriction. If the magnitude of saturation magnetostriction is known, it is possible to explain the anomalies in permeability and coercive force[9].

There are main three reasons for studying the magnetostriction [12].

1. A study may throw light on the nature and behaviour of the special internal forces in a ferromagnetic material.
2. By utilizing the phenomenon of magnetostriction, an electrical pulse can be converted into mechanical one and vice versa. This enables it to be used for the production of magnetostriction oscillators, filters of very high stability and electrochemical transducers, particularly for obtaining high intensity ultrasonic waves.
3. In investigating magnetization processes and analyzing the magnetization curve.

For cubic ferrites, only change occur in volume whereas in hexagonal ferrites, the change occurs in volume as well as in shape. These changes occurs even when the sample is cubic but magnetic order is noncubic. This behaviour is due to dependence of exchange energy on interatomic spacing. A comprehensive review of magnetostriction is given by Lee[10] and Briss [11].

S.R.Murthy and T.S. Rao [12] studied the magnetostriction of polycrystalline mixed nickel -zinc and cobalt-zinc ferrites as a function of composition, magnetic field and temperature using the strain gauge method. They observed that the values of saturation magnetostriction in both the ferrite systems decreases with increase of zinc concentration. They explained the anomalous bahvaiour observed in the variation of magnetostriction with temperature on the basis of magnetic anisotropy energy.

5.2 Weiss Domain structure

Ferromagnetic and ferrimagntiec substances exhibit a spontaneous magnetization even in the absence of an external magnetic field. However, even the application of a small magnetic field usually produces a large magnetization. The appearance of a large magnetization is explained by Weiss [13] by postulating the existence of the small regions, called domains, each of which is fully magnetized. The magnetic moments within such region are aligned in the same direction. In domains the magnetization vectors are parallel to preferred direction such that the demagnetizing field results into lower energy. The influence of Weiss domain structure on the resonance condition is studied by Snoek [14]. According to him, resonance is also possible in a non saturated specimen i.e. in a specimen still divided into Weiss domains. Polder and Smith [15] reported that the Weiss domain structure in demagnetized samples affects resonance behaviour. In general, the switching dynamics can be explained on the basis of theory of damping of moving domain boundary [16].

5.3 Bloch wall

In the unmagnetized state of solid, the spins of Weiss domains are oriented at random. There is transition of spin directions from one domain to another. This transition does not take place abruptly but extends over a certain width of boundary is known as domain wall or Bloch wall. The domain wall has a finite thickness and structure which can be determined by the number of

lattice distances transversed to produce transition. The Bloch wall energy is lower when the exchange is distributed over many spins.

If ϕ is the angle between the spins in the successive atomic layers then the exchange energy between them is given by,

$$w_{ex} = Js^2 \phi^2 \qquad \ldots 5.1$$

The exchange interaction tends to make a wall as thick as possible. The spin contained within the wall are largely directed away from the axis of easy magnetization. Therefore, there is an anisotropy energy associated with the wall. The wall energy is roughly half the exchange energy.

Magnetic domain behaviour of $MgFe_2O_4$-$CoFe_2O_4$ system was studied by Rao V and Keer H. V. [17] to elaborate the multidomain and single domain grains.

5.4 Domain wall thickness

A formula for estimating domain wall thickenss (t_w) in a bulk material is given by [18].

$$t_w = a \sqrt{Js}\, [3KTc/2n_B\mu_\beta K_1]^{1/2} \qquad .... 5.2$$

Here a is the distance between nearest dipoles, Js is the saturation intensity, K is the Boltzmann constant, Tc is a Curie temperature, n_B is the magneton number per formula unit, μ_β is the Bohr magneton and K_1 is the anisotropy constant for the material. This formula is derived for ferromagnet and

errimagnets. Domain wall thickness (t_w) mainly increases with increasing exchange interaction and reducing anisotropy.

The typical domain wall thickness is about $10^3 A^o$ (10^{-07}m) and the associated energy is about 10^{-3}J/m^2[19].

5.5 Domain state and hysteresis loop

The demagnetized state of a ferro or ferrimagnetic body is normally presumed to be due to the sub-division into Weiss domain with Bloch walls between them.

A polycrystalline ferrimagnetic material may consist of three types of domain states.

1. Multidomain (MD)
2. Single domain (SD)
3. Super - paramagnetic (SP) state.

Grains which have domain walls in them are known as multidomain (MD). Thickness of these grains is found to be in the range of a few hundred to few thousands angstrons for different materials.The grains can not contain walls due to energy consideration method termed as single domain for which the magnetization direction is fixed in space. If the thermal energy of the SD grains is comparable to the effective magnetic anisotropy energy, then the magnetization of the grains undergo fluctuations and the grains are in super-paramagnetic state [20]. As reported by Neel [21] magnetostatic energy of single domain (SD) particles is given by

$$vJsHc = 2kT_b \quad \text{.... 5.3}$$

where K - Boltzmann constant

T_b - blocking temperature

H_c - Coercive force

v - volume of grain

J_s - Saturation intensity.

Hence, the magnetic states of single domain and super-paramagnetic are interchangeable by temperature.

Radhakrishana Murthy et al [22] have shown that normalized χ_{ac}-T curves and hysteresis loops of micropowders consisting of different domain states of ferromagnet related with each other. They have shown that susceptibility for a multidomain sample does not change appreciably with temperature and drops off sharply at the Curie point (Tc). But in χ_{ac} - T_c curves of a single domain sample, there could be broad hump below T_c or sharp cusp near Tc depending upon the temperature at which the single domain becomes superparamagnetic.

For SD state, two types of hysteresis loops are possible.

1. One for randomly oriented grains with dominant uniaxial anisotropy (SD - UA), for which the remanent intensity will be one half of saturation intensity and

2. The other for grains with more than one pair of easy axes which will be the case when magnetocrystalline anisotropy dominates (SD-CA), for which

the ratio of remanent and saturation intensity will be 0.8 or more and hence the hysteresis loop will be more square in nature.

According to Bean [23], coercive field (H_c) and remanent intensity is very small for MD samples whereas for SD particles these are considerably large. Schematic hysteresis loops and normalized susceptibility versus temperature curves for sample consisting of different domain state are shown in Fig. 5.1.

5.6 Temperature dependent initial susceptibility

The apparent susceptibility χ is related to the real susceptibility χ' by the relation [21].

$$\chi = \frac{\chi'}{(1+N\chi')} \qquad \text{..... 5.4}$$

where N is the demagnetization factor.

A.C. susceptibility measurement in a field of 0.5 Oe by double coil method carried out on magnetite by Radhakrishnamurthy et al [24] and showed that there are three types of susceptibility peaks in the χ_{ac} - T curves

1. Isotropic peak occurs only if the magento crytalline anisotropy is zero for a magnetic material in MD form.

2. Hopkinson peak, just occurring before the T_c of any magnetic material in multidomain state.

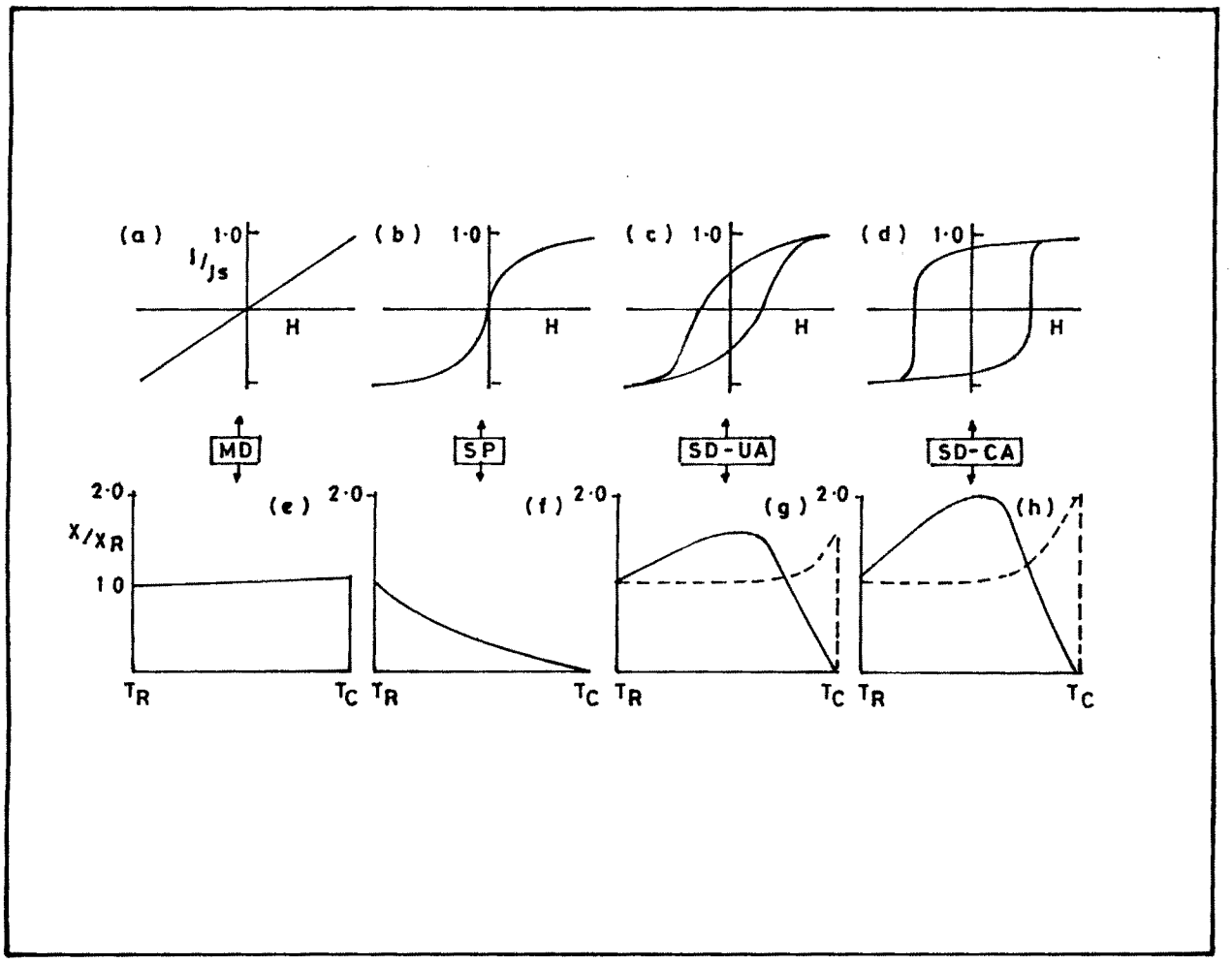

FIG.5·1 - SCHEMATIC HYSTERSIS LOOPS AND NORMALIZED SUSCEPTIBILITY VERSUS TEMPERATURE CURVES FOR SAMPLE CONSISTING OF DIFFERENT DOMAIN STATES.

3. Single domain peak occurs at T_b only if the sample has substantial proportion of SD particles.

The variation of (χ_T/χ_{RT}) for the magnetite having MD and SD grains is shown in Figure 5.2 [24].

5.7 Magnetocrystalline anisotropy energy

An energy in a ferromagnetic crystal which directs the magnetization along certain definate crystallographic axes is called magnetocrystalline anisotropy energy.

The crystalline anisotropy can be described by the first two or three terms of infinite power series in the direction cosine of the magnetization vector with respect to the crystal axes. For cubic crystal such as iron, anisotropy energy is given as

$$E_{an} = k_1(\alpha_1^2\alpha_2^2 + \alpha_2^2\alpha_3^2 + \alpha_3^2\alpha_1^2) + k_2(\alpha_1^2\alpha_2^2\alpha_3^2) + \ldots\ldots\ldots 5.5$$

where k_1 and k_2 are the first and second anisotropy constants α_1, α_2 and α_3 are the direction cosines. Anisotropy constant k_1 and k_2 at room temperature are determined by neglecting higher terms in above equation

$K_1 = 4.2 \times 10^5 \text{erg/cm}^3$ and $k_2 = 1.5 \times 10^5 \text{ erg/cm}^3$.

Anisotropy energy for a crystal with a single preferred axes, such as cobalt may be written as

$$E_{an} = k_1\sin^2\phi + k_2\sin^4\phi \qquad \ldots\ldots 5.6$$

where ϕ is the angle between magnetization and easy axis.

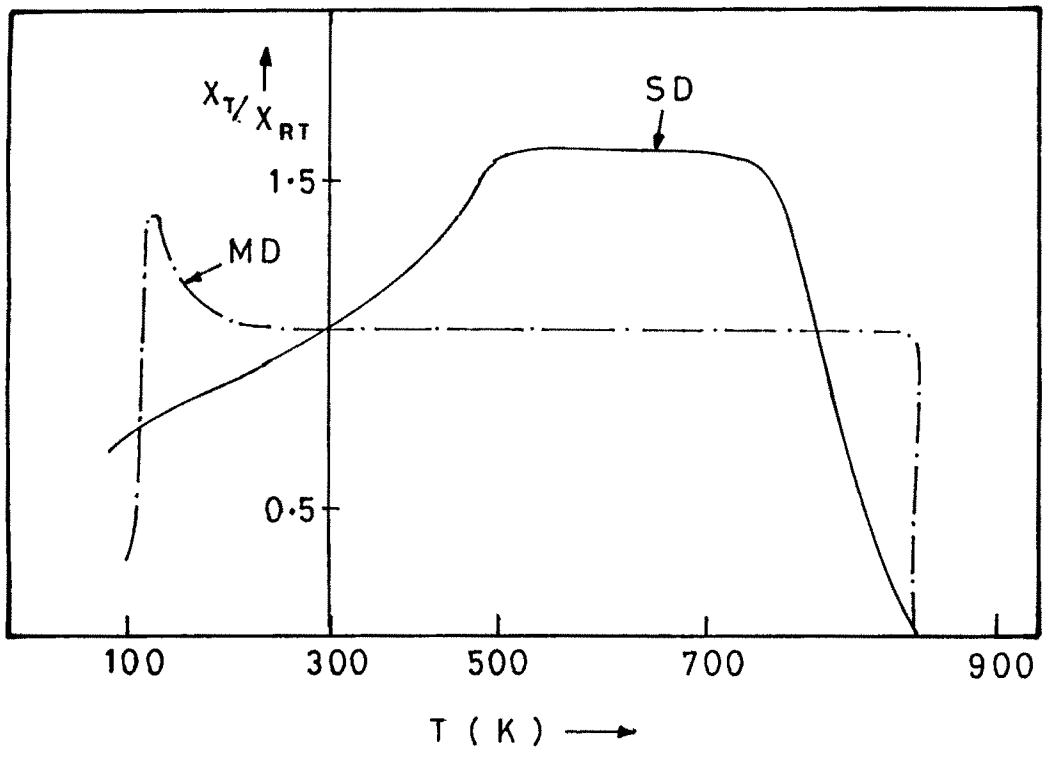

FIG.5·2- VARIATION OF NORMALIZED SUSCEPTIBILITY WITH TEMPERATURE FOR THE MAGNETITE.

At room temperature k_1 and k_2 are found to be $k_1 = 4.1 \times 10^6$ ergs /cm^3 and $k_2 = 1.0 \times 10^6$ ergs/cm^3.

It should be noted that, anisotropy energy strongly depends on temperature. In many ferrites K_2 is very small as compared to K_1.

Several investigators [25-31] determined the anisotropy constants of ferrites.

Magnetocrystalline anisotropy in single crystals of magnetite and in cobalt substituted are examined by Bickford and his co-workers [32].

5.8 Magnetization process

When the applied filed across the demagnetized specimen is small enough, the induced magnetization varies linearly with the field and is also reversible. However, when the field is steadily increased, the magnetization process becomes irreversible. The plot of change of magnetization with applied field H is called hysteresis loop as shown in Figure 5.3.

With increasing field from zero, the magnetization steadily increases and attains a saturation value for a particular value of field. This maximum saturation value is called the spontaneous magnetization (Ms). A further increase in the field does not produce any further change in the spontaneous magnetization.

However, when the field is decreased, magnetization decreases but follows another path and when the field is reduced to zero, a certain amount

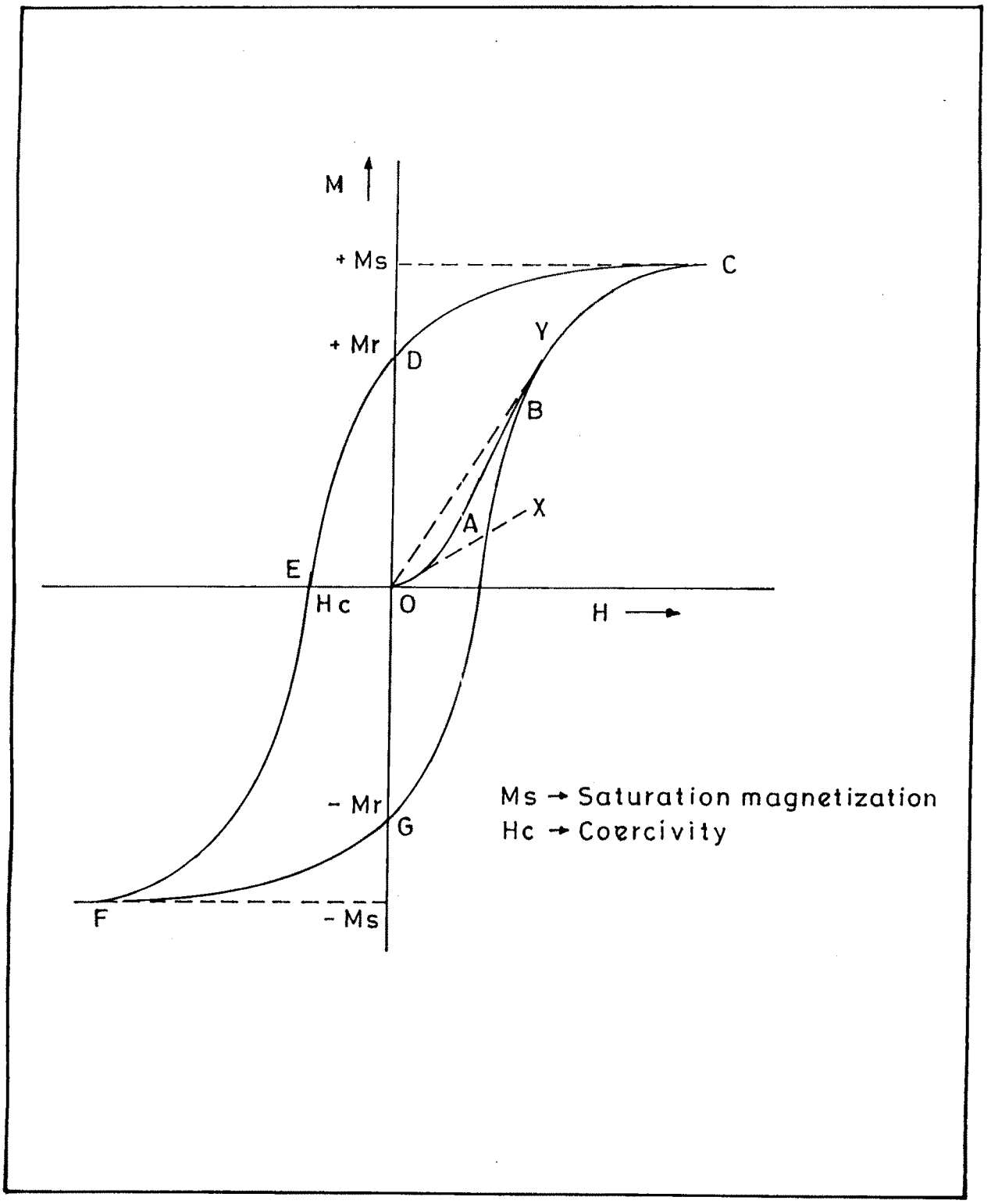

FIG. 5·3— HYSTERSIS LOOP (CDEFGC).

of magnetization is still retained by the sample. This is called remanent magnetization (M_r).

Further, when the applied field increases in opposite direction, magnetization decreases and for a particular value of field it becomes zero. The magnitude of the field, which completely reduces the magnetization to zero is called coercive force.

If the field is further increased in opposite direction, the sample gets saturated in the opposite direction. Finally, if the field is reversed, a loop called hysteresis loop is obtained.

The magnitude of initial susceptibility is obtained by drawing the tangent ox to magnetization curve and measuring its slope. The value of maximum susceptibility is obtained by slope of the line OY in the knee part of magnetization curve.

5.9 Losses in ferrites

Hysteresis loss, eddy current loss, relaxation loss, spin resonance loss and wall resonance loss are the significant losses in the ferrites.

a) Hysteresis loss

Hysteresis loss is due to irreversible wall displacements. This loss increases with grain diameter and with the impurity content of raw materials. This loss does not appear in the initial permeability, because a finite field amplitude is required. For small amplitude, the hysteresis loss is proportional to the amplitude and is described by the relation

$$\frac{(\tan\delta)_{hysteresis}}{\mu} = \frac{a_h B_{max}}{2\pi} \qquad \text{..... 5.7}$$

where a_h = amplitude

B_{max} - maximum induction in the core

μ - permeability

In technical applications, an important effect of hysteresis loss is a distortion of signal proportional to $(\tan\delta)_{hysteresis}$.

b) Eddy current loss

Under the action of alternating magnetic field, an electric current is induced in the magnetic core material. This causes heating and power loss. The power loss interms of frequency and resistivity is given by

$$p = A(f^2/\rho) \qquad \text{.... 5.8}$$

where f - is the frequency of applied field.

ρ - is the electrical resistivity of the core material

A - is the proportionality constant which depends on the shape of the core.

In cores, the corresponding eddy current losses are given by the equation

$$\frac{(\tan\delta)_{eddy}}{\mu} = 2 \times 10^{-5} f \qquad \text{.... 5.9}$$

where frequency 'f' is expressed in MHz.

c) Relaxation loss

These losses occur at frequencies much lower than the resonant frequency and have significant contribution to the magnetic losses.This loss is found in ferrite due to exchange of electron between divalent and trivalent iron ions, when the magnetization changed its direction, Fe^{2+} and Fe^{3+} ions change their positions and attain new configuration that has the lower energy under the changed direction of magnetic field. The readjustment of ferrous and ferric ions do not requires the movement of ions, but only requires transfer of electrons.The relaxation loss depends on the frequency and is maximum when the applied frequency becomes equal to relaxation frequency for electron jump.

For Ni-Zn ferrites fired at high temperature, the relaxation frequency is of the order of $3x10^8$Hz, whereas for the Ni-Zn ferrites fired at low temperature, the relaxation frequency is much higher being about 10^{13} Hz[33].

d) Spin resonance loss

This loss is due to the natural resonance of rotation of magnetization in the presence of restoring torque developed by the anisotropy field. The precessional frequency ω of an electron spin vector in presence of internal anisotropy filed H_k is given by

$$\omega = 2\pi f_y = \gamma H_k. \qquad \text{.... 5.10}$$

Where γ - gyromagnetic ratio.

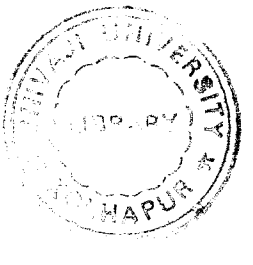

H_k - is the internal anisotropy field and is perpendicular to external magnetic field Hi. When the frequency of external magnetic field matches the precessional frequency, resonance occurs and energy is absorbed from the applied field and dissipated in the material. The rotational process is important for a material having negative anisotropy constant and is found to be inversely proportional to (μ-1). Hence higher the permeability lower is the resonance frequency and vice versa.

e) Wall resonance loss

In certain ferrites, the domain wall resonance loss occurs at low frequency. If the domain wall is distributed from its equilibrium position, restoring force developes in the wall which tries to bring it back to its original position. Thus the domain wall behaves as stretched elastic membrane having some natural frequency of oscillation. As the frequency of applied filed equals the natural frequency of domain wall, resonance absorption set in.

5.10 Curie temperature

Ferromagnetic or ferrimagnetic substances consist of small zones or regions called domain which posses magnetic moments when the spins of the atoms in them are aligned parallel to each other. At 0^{o}K, spin ordering is due to strong internal magnetic field. Therefore, at absolute zero the spontaneous magnetization is maximum. As temperature increases, the thermal agitation opposes this spin alignment and at a certain temperature called Curie temperature the spontaneous magnetization disappear.

The Curie temperature Tc is given as

$$Tc = \frac{2\,S\,(S+1)\,Z\,J}{3K} \qquad \text{.... 5.11}$$

where K- Boltzmann constant

S- spin angular momentum

Z- number of nearest ions

J - total angular momentum.

From above equation, it is clear that Curie temperature increases with increasing s for constant interaction per spin and magnetization of the ions posses more than one uncompensated spins, the Curie temperature is higher when these spins are coupled in one spin. Curie temperature depends on the distribution of cations on tetrahedral and octahedral sites [34-35]. Gilleo [36] theoretically estimated the values of Curie temperature for substituted spinel ferrite by using statistical model.

$$Tc(k_0, k_1) = \frac{3\,n\,(K_0,K_t)}{24\,N(K_0, K_t)}\; Tc\,(0,0) \qquad \text{.... 5.12}$$

Here Tc(0,0) is the Curie temperature of unsubstituted ferrites

$n(K_0,K_t)$ - active magnetic interaction per formula unit.

$N(K_0,K_t)$ - denotes the number of magnetic ions actively participating in the ferrimagnetism.

K_0, K_t - are the fractions of ions substituted on octahedral and tetrahedral sites

According to Gilleo, Curie temperature in ferrimagntiec material is found to be proportional to number of active magnetic linkage. This model is applicable only when all magnetic ions are identical or when the substituted ion displaces a magnetic ion on the same site. Upadhyay [37] suggested a simplified model to calculated Curie temperature of ferrimagnetic spinels by using equation

$$Tc(x) = \frac{M^*(x=0.0)n(x)}{M^*(x)\, n(x=0.0)} \quad Tc(x=0) \qquad \ldots\ldots 5.13$$

where M* (x=0.0) is a dimensionless parameter

n(x) - number of relative weighted magnetic interaction per formula unit.

This model is valid for any substituted ferrite. Valenzueia [38] reported a sensitive method for the determination of the Curie temperature of Ni-Zn ferrites based on the technique of continuos measurement of initial magnetic permeability and compared it with the values of Curie temperatures obtained from differential scattering calorimeter.

Ghatage et al [6] recently reported the values of Curie temperature of Ti substituted Ni-Zn ferrites obtained from Gilleo's model and a.c. susceptibility measurement. Sawant et al [39] reported the values of Curie temperature of Co-Zn ferrites obtained from Gilleo's model, a.c. susceptibility measurement and Loria-Sinha technique. Several investigators obtained the

values of Curie temperatures from D.C. resistivity [40-43] a.c. susceptibility [44-49] and permeability [50-54] measurements and Upadhyay model [55,56].

Part A : Hysteresis

5.A.1 Experimental

Magnetization measurement of the sample in the series $Ni_{1-x}Zn_xFe_2O_4$ were carried out with the help of high field loop tracer operating at 230 volts, 50 Hz mains frequency [57].

The circuit diagram of hysteresis loop tracer is as shown in Fig. 5.4

It consists of an electromagnet. The variable alternating magnetic field is produced in an air gap of about 1 cm width in the instrument. The specimen is placed in a special balancing coil and inserted in the gap.Depending upon the magentic induction in the specimen, pick up coil produces a field. Simultaneously the supporting coil produces a signal equivalent to the strength of magnetic field. When respective signals are supplied to the vertical and horizontal deflecting plates of oscilloscope, hysteresis loop is visible on the screen. The vertical displacement corresponding to saturation magnetization of hysteresis on screen is calibrated by placing a small nickel sample between the two pole pieces. The mass of nickel sample used in the present case is 1.026 gm and the vertical displacement was equivalent to R = 5.2 division on CRO. The magnetic moment of pure nickel sample is 53.34 emu/gm.

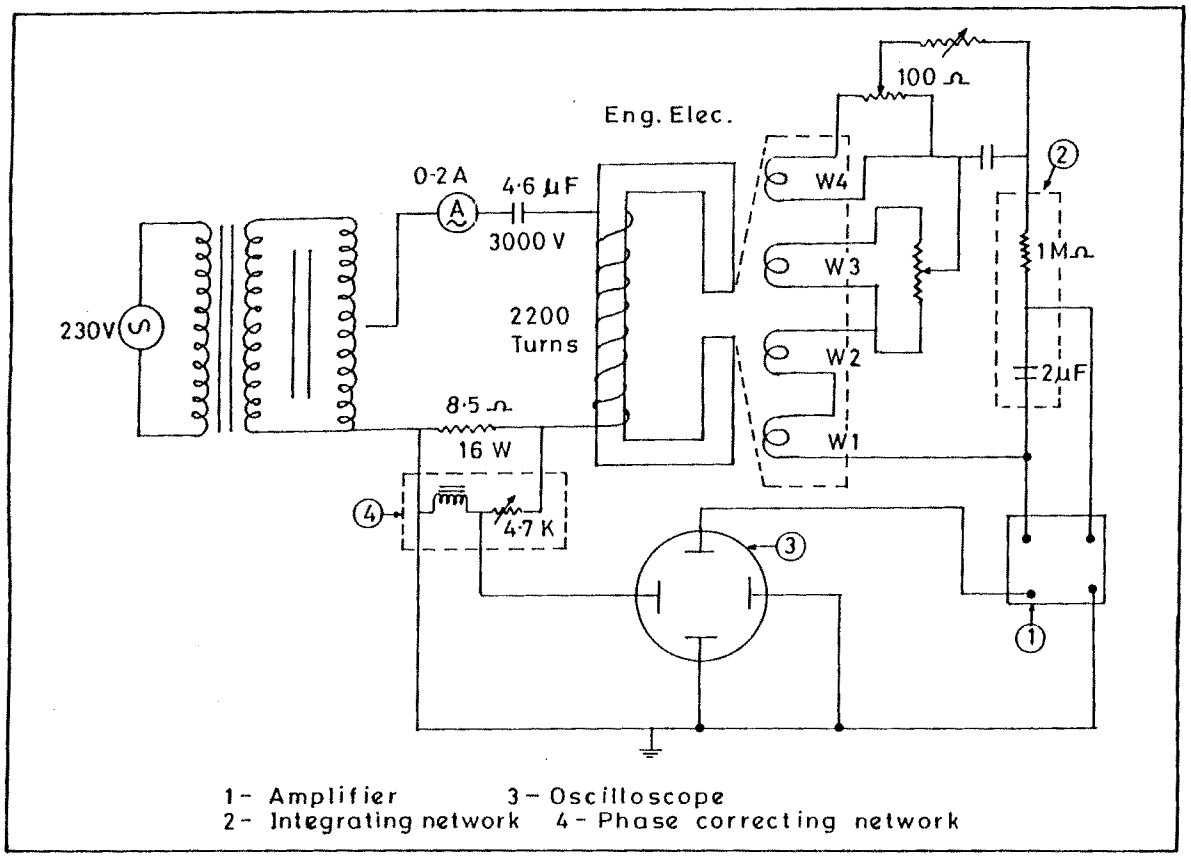

FIG. 5·4 — THE CIRCUIT DIAGRAM OF HYSTERSIS LOOP TRACER.

Hence total magnetization of nickel is

$$X = 54.7268 \text{ emu}$$

Therefore the calibration factor comes out to be

$$C.F. = X/R$$

$$= 10.5243 \text{ emu/div}$$

The procedure was repeated for other samples under investigation. The vertical displacement corresponding to all the samples were recorded and saturation magnetization was calculated using the relation,

$$\sigma_s = \text{(vertical displacement) x (calibration factor)}$$

Hence, the magnetization per unit mass is

$$\sigma'_s = \frac{\sigma_s}{\text{Mass of pellet}} \text{ emu / gm} \qquad \text{.... 5.14}$$

The saturation magnetization (Ms) is given by the relation

$$Ms = (1-p)\ \rho_x \sigma'_s \quad \text{(gauss)} \qquad \text{....5.15}$$

where ρ_x - x-ray density, p - porosity

The magnetic moment (n_β) was calibrated as

$$n_\beta = \frac{\text{(mol.wt) x (saturation magnetization)}}{55.85} \text{ (Bohr Magneton)} \qquad \text{..... 5.16}$$

5.A. 2 Results and discussion

Hysteresis loops for pure nickel and $Ni_{1-x}Zn_xFe_2O_4$ (x= 0, 0.20, 0.40, 0.60 and 0.80) samples recorded at room temperature are presented in figures 5.5 and 5.6.

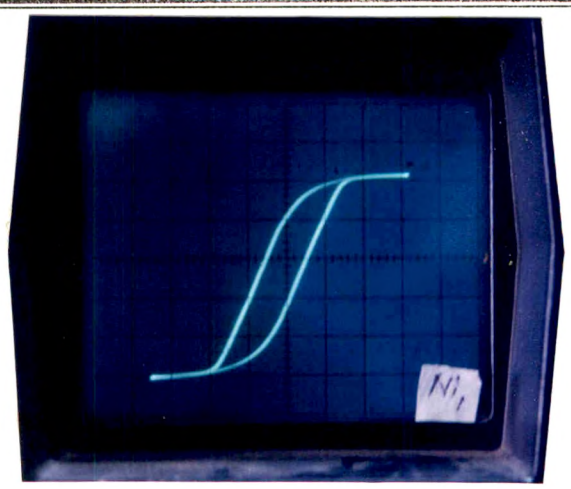

Pure Nickel Sample

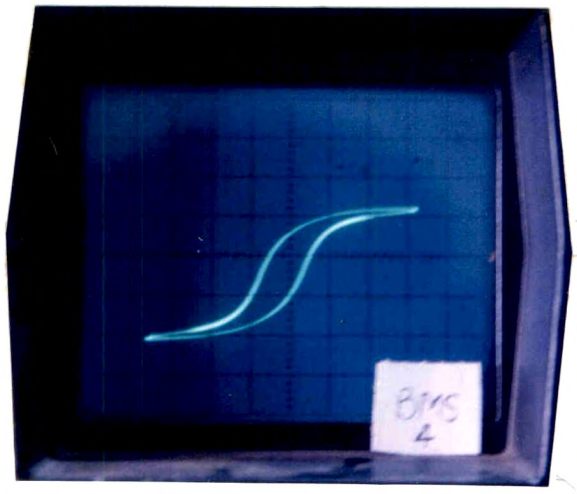

X= 0

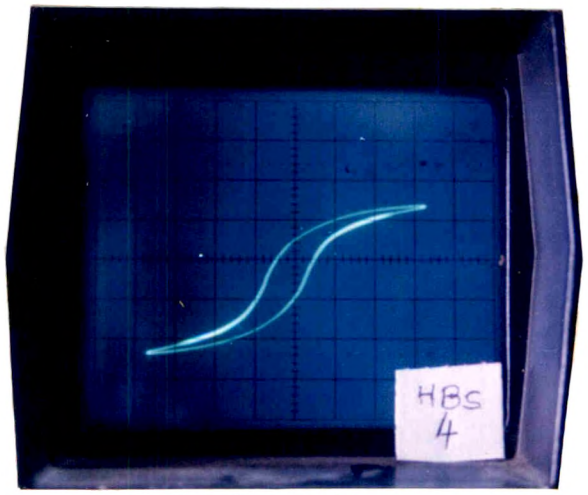

X = 0.20

Fig. 5.5: Hysteresis loop for pure nickel sample & $Ni_{1-X}Zn_XFe_2O_4$ (X= 0, 0.20).

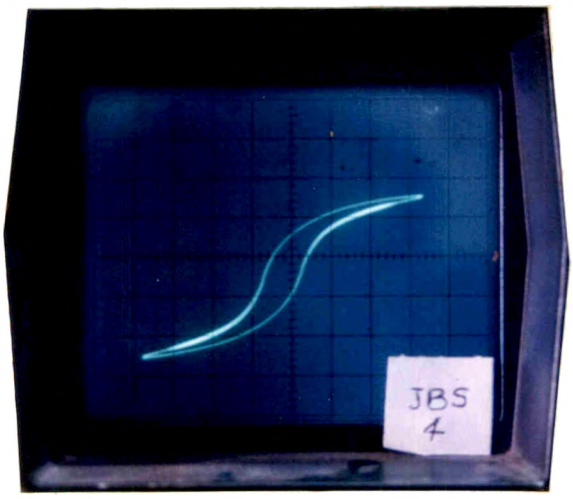

X = 0.40

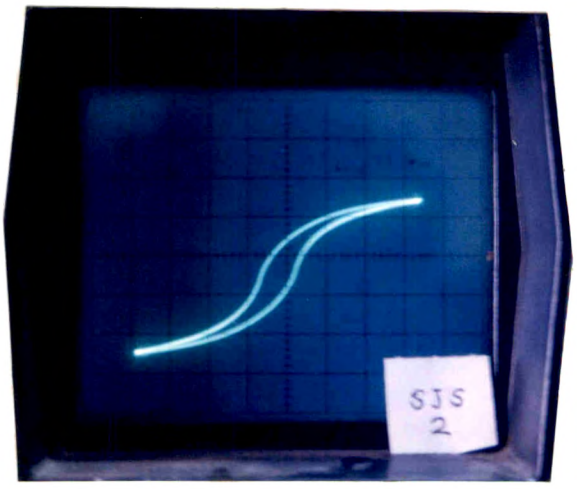

X = 0.60

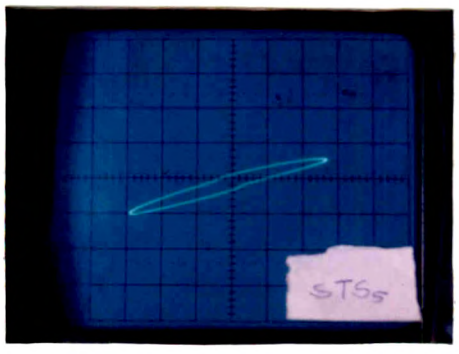

X= 0.80

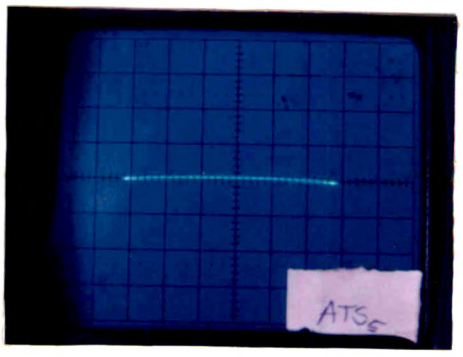

X= 1.00

Fig. 5.6: Hysteresis loop for $Ni_{1-X}Zn_XFe_2O_4$ (X= 0.40, 0.60, 0.80, 1.00).

The values of saturation magnetization σ'_s , $4\pi M_s$ and magnetic moment n_β are obtained from figures 5.5 and 5.6 and the relations 5.15 and 5.16 and are presented in Table 5.1.

Table 5.1

Magnetization data of $Ni_{1-x}Zn_xFe_2O_4$ system

Zinc content x	**Saturation magnetization**		**Magnetic moment n_β (Bhor magnetron)**	**Y-K angles (Degree)**
	σ'_s (emu/gm)	**4ΠMs (Gauss)**		
0	45.59	3054	1.90	0
0.20	59.13	3915	2.50	0
0.40	68.23	4519	2.90	22°53'
0.60	58.51	3895	2.49	47°3'
0.80	17.87	1190	0.77	74°56'
1.00	-	-	-	90°

From this table, it is observed that the value of ($4\pi M_s$) is minimum for $NiFe_2O_4$ and $Ni_{0.2}Zn_{0.8}Fe_2O_4$ and maximum for $Ni_{0.6}Zn_{0.4}Fe_2O_4$. The variation of σ'_s and $4\pi M_s$ with the content of zinc are shown in figures 5.7 and 5.8. From figure 5.7, it is observed that, saturation magnetization increases with increasing concentration of zinc upto x=0.40 and then falls off with increasing in zinc concentration [58]. Similar result is reported by Daniels and

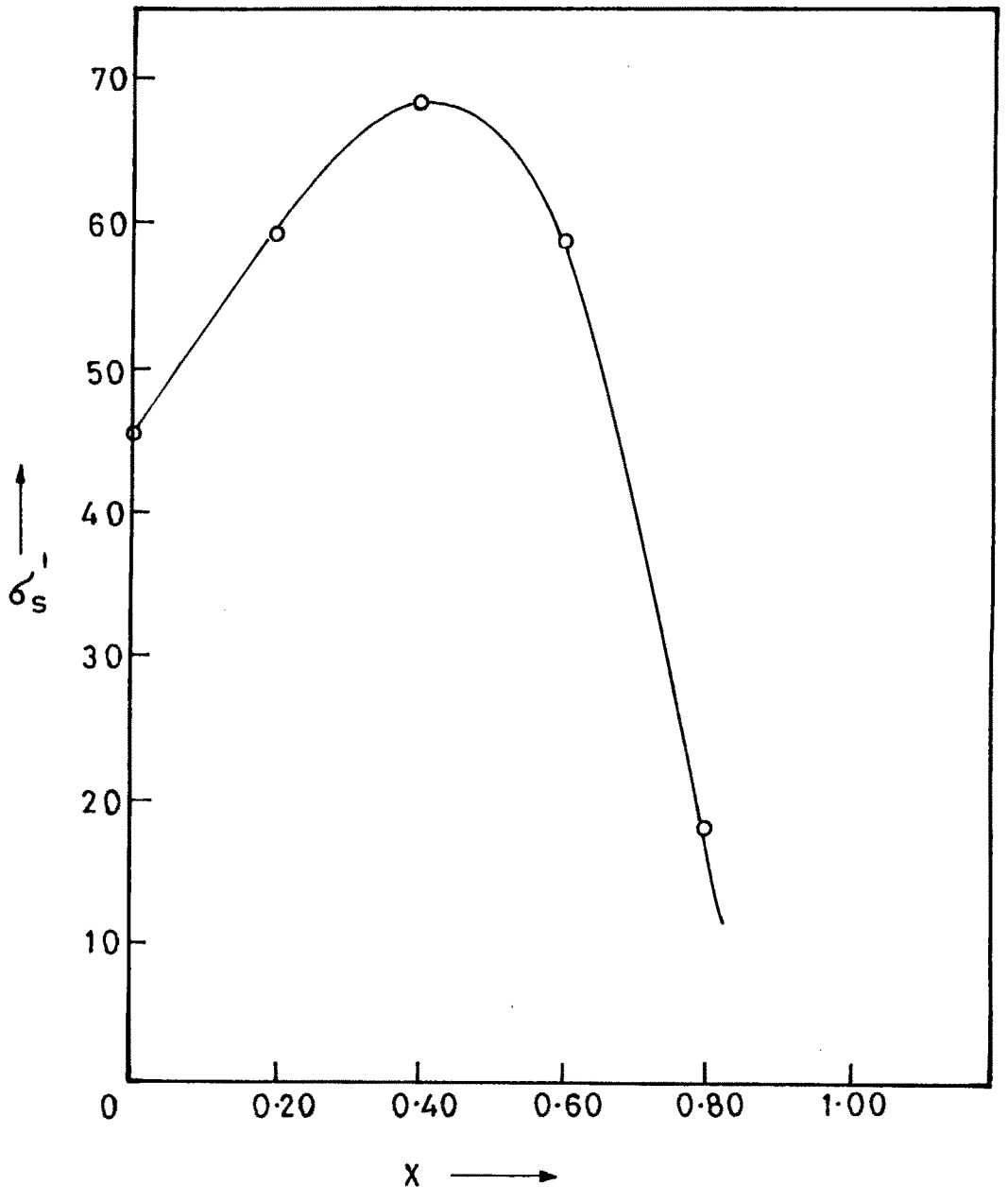

FIG. 5·7 - VARIATION OF SATURATION MAGNETIZATION (σ_s') WITH ZINC CONCENTRATION.

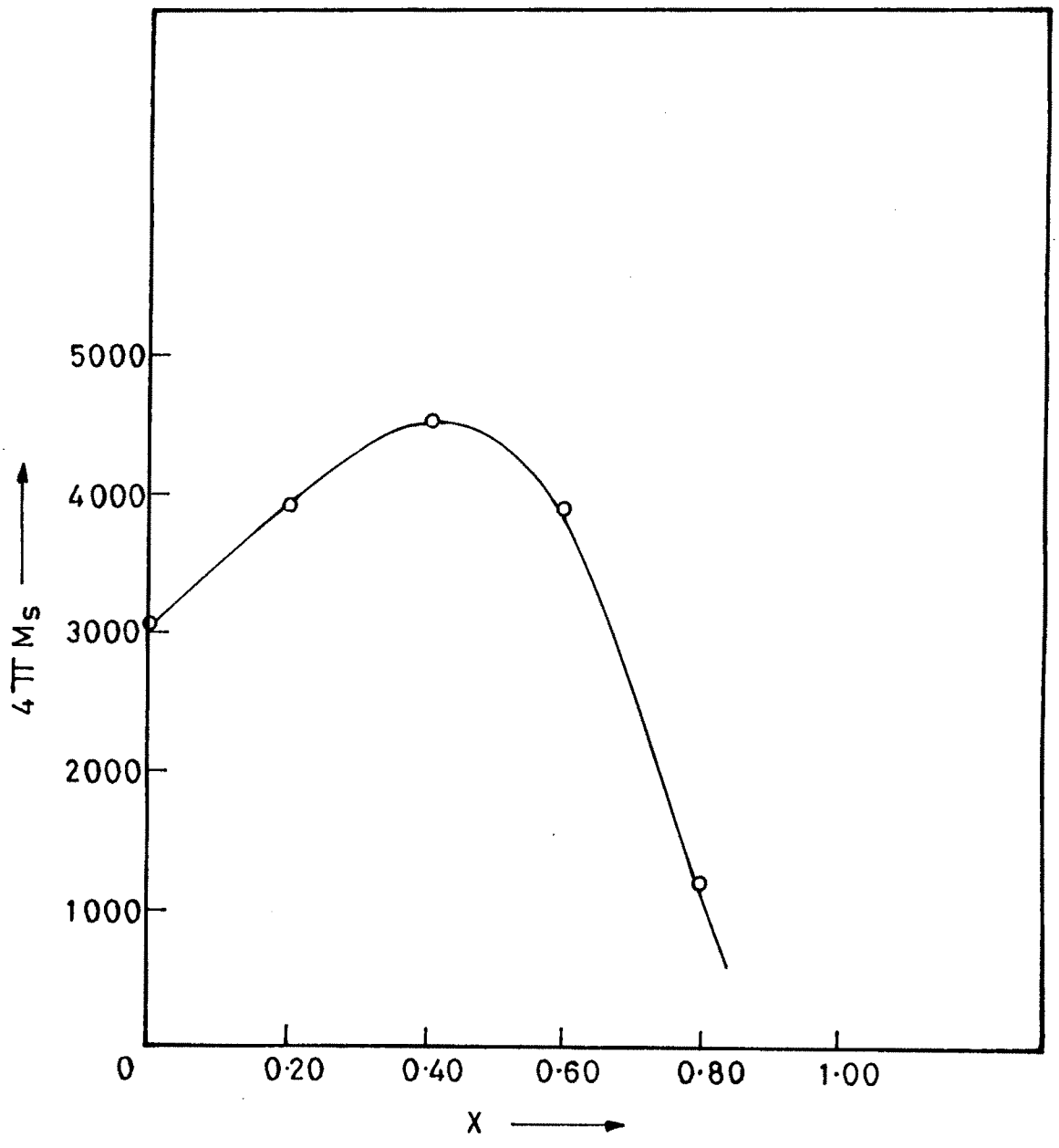

FIG.5·8 - VARIATION OF MAGNETIZATION (4 π Ms) WITH ZINC CONCENTRATION.

Rosenwaig [59] for Ni-Zn ferrites prepared by ceramic method. Mossbauer study of Ni-Zn ferrites [59] yields the cation distribution as

$$(Zn_x^{2+} Fe_{1-x}^{3+})^A [Ni_{1-x}^{2+} Fe_{1+x}^{3+}]^B$$

It shows that all the Zn^{2+} ions occupy tetrahedral sites(A) and Ni^{2+} ions occupy octahedral sites (B) and Fe^{3+} ions distributed along tetrahedral and octahedral sites respectively.As the content of Zn^{2+} ions increases, Fe^{3+} ions migrating to B sites increase, thus increasing M_B and decreasing the M_A. Therefore the net value of saturation magnetization increases. When the value of x exceeds 0.40, saturation magnetization starts decreasing because magnetic moment of the few remaining Fe^{3+} ions on the A site are no longer able to align all the moments of the B sites antiparallel to themselves since this opposed by the negative B-B exchange interaction [60].

Figure 5.9 shows variation of magnetic moment (n_β) with zinc content. Similar variation of n_β with zinc content has been also observed in other zinc substituted ferrites like Ni-Zn [61], Co-Zn [62], Mn-Zn [63] and Mg-Zn[64].

According to Gilleo [37], variation of n_β in the Ni-Zn ferrites arise due to the presence of super-paramagnetic clusters or paramagnetic centers formed due to insufficient magnetic linkages.

Low temperature Mossbauer studies by Leung et al [65], neutron diffraction studies by Staya Murthy et al [2] and ferromagnetic relaxation studies by Srivastava and Patni [3] do not support the cluster model.

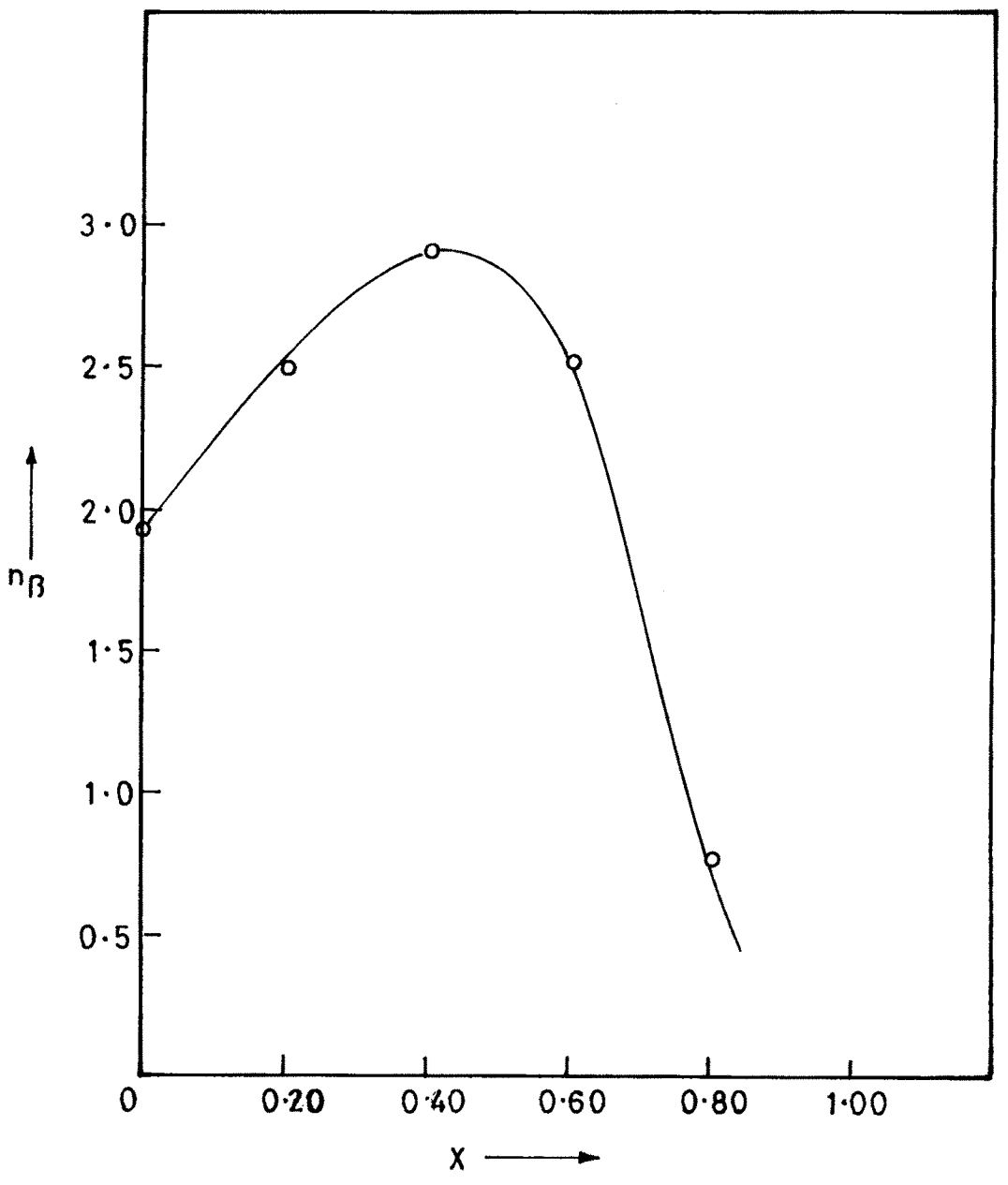

FIG. 5·9 - VARIATION OF MAGNETIC MOMENT WITH ZINC CONCENTRATION.

On the basis of neutron diffraction measurements, Satya Murthy et al [2] believed that the change in magnetization of zinc substitution occurs due to the presence of Y-K angles in the spin system on the B- site and is later confirmedd by a number of workers [59, 65].

The condition for the existence of Y-K angles in the Ni-Zn system has been investigated in the molecular field approximation by Satya Murthy et al [2] using a non-collinear three sublattice model. Srivastava et al [66] have studied magnetic ordering and domain wall relaxation in zinc ferrites. They have calculated theoretical values of Y-K angles using the formula

$$\cos\alpha_{yk} = \frac{10(1-x)^2\alpha + 25\,(1-x^2)\,\beta}{16(1-x)^2\,\gamma + 25\,(1-x)^2\delta + 40(1-x^2)\,\varepsilon} \qquad \text{....5.17}$$

The molecular field constants, α, β, γ, δ and ε can be obtained from the observed variation of saturation magnetization with zinc concentration. They have used the values of exchange constants as follows

$J_\alpha = -21$ K $\qquad J_\beta = -28$ K

$J_\delta = -10$ K $\qquad Jy = -64$ K

and $J_\varepsilon = -24$ K

The variation of saturation magnetization with zinc concentration is related by the relation

$$n_\beta = (9+x)\cos\alpha_{yk} - 5(1-x) \qquad \text{..... 5.18}$$

where n_β is expressed in units of Bohr-magneton.

The Y-K angles in the present system are calculated by using the formula [65].

$$n_\beta = (6 + x)\cos\alpha_{yk} - 5(1-x) \quad \text{..... 5.19}$$

where x is the content of zinc

The values of Y-K angles are also presnetd in table 5.1. From this table, it is observed that Y-K angles for the composition x=0. and x=0.20 are zero, suggesting that the existence of Neel's two sublattice model. The occurrence of Y-K angles for the compositions $x \geq 0.40$ suggesting the existence of Y-K model. It is also observed that, the Y-K angles increases with increases in zinc content.The increasing Y-K angles indicates the more favoring of triangular spin arrangements on B-site leading to reduction in A-B interaction.For zinc ferrite $\cos\alpha_{yk} = 90^o$, suggesting that B-B interaction collapses leading to zero saturation magnetization. Similar result have reported by Joshi et al [67] for the Ni-Zn ferrites prepared by ceramic method.

The reported values of saturation magnetization of the composition 0.40 , prepared by ceramic [68] and citrate [69] methods are about 60 emu/gm and 63 emu/gm respectively. Whereas the value of same composition prepared by present method is improved upto 68.23 emu/gm. The ferrites prepared in the present method have high density. The porosity of this sample lie in the range 1.18 % to 2.5 %. Therefore the saturation magnetization is improved as compared to ceramic and citrate precursor method. High resistivity Ni-Zn ferrites by citrate precursor method, has studied by Verma et al [69]. They

have shown the remarkable increase in value of saturation magnetization for the composition $Ni_{0.4}Zn_{0.6}Fe_2O_4$ as compared to ceramic method. Electrical and magnetic properties of normal and hot pressed Mn-Zn ferrites are studied by Puri et al [70]. They observed marked increase in the values of saturation magnetization for hot pressed ferrite than those of normal ferrite with the same composition. They attributed the higher values of saturation magnetization to very low porosity of hot pressed ferrites.Bhosale et al [71] have studied the synthesis of high permeability Cu-Mg-Zn ferrites using oxalate precursors and showed that the values of saturation magnetization are improved as compared to ceramic method.

Part B Curie temperature

5.B.1 Experimental

The Curie temperature measurement of $Ni_{1-x}Zn_xFe_2O_4$ system in the form of the pellets of different composition was carried out by using Loria - Sinha technique [72]. The schematic diagram of its setup is shwon in Figure 5.10.

The apparatus consist of specially designed cylindrical furnace having circular aperture along its axis. An electromagnet operated at 1.5 Ampere and 15 Volt is held vertically along the axis of furnace, just above its top. Lower end of the electromagnet insulated by porceline sheet in order to avoid the direct heat from the furnace. A nail type soft iron rod introduced into the furnace holds the field of electromagnet. A ferrite sample whose Curie

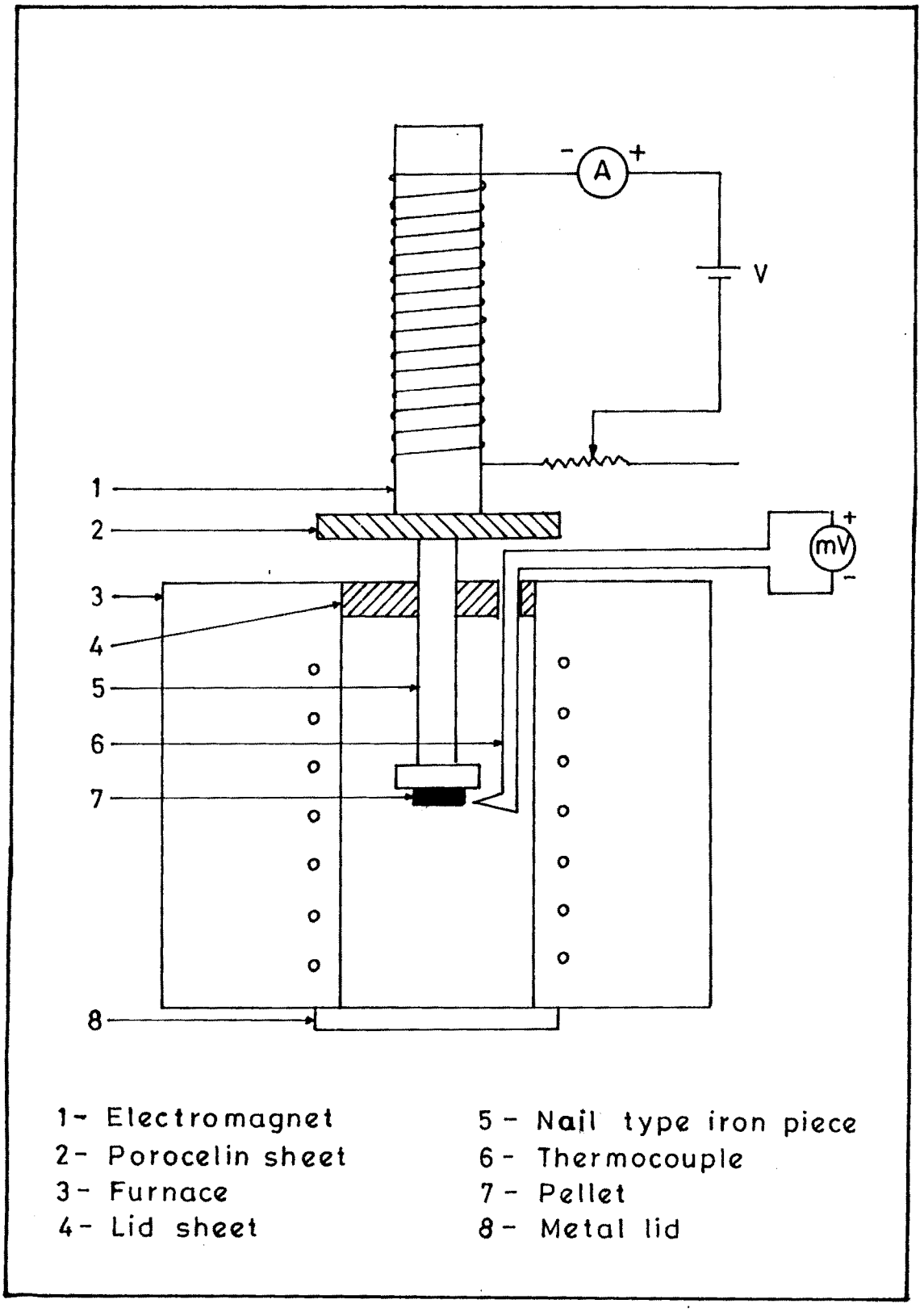

FIG. 5·10 – SCHEMATIC DIAGRAM OF CURIE TEMPERATURE SET-UP.

temperature is to be determined is kept at the top of elbow type rod and is introduced vertically upward. The sample gets attracted to the nail and is attached to it. To measure temperature of furnace, a chromal-alumel thermocouple introduced in the furnace with its junction position very near to the position of the pellet. The temperature of the furnace can be increases slowly by using dimmerstat. At particular temperature sample losses its magnetization and gets detached from the electromagnet and falls down giving Cuire temperature.

5.B.2 Results and discussion

The Curie temperature of $Ni_{1-x}Zn_xFe_2O_4$system (x= 0, 0.20, 0.40, 0.60 and 0.80), obtained from Loria-Sinha technique is presented in Table 5.2. From this table, it is observed that Curie temperature decreases with increasing zinc content. The decrease in Curie temperature with zinc content is attributed to decrease of AB interaction. As the content of zinc is increased, the relative number of Fe^{3+} ions on A site decreases, which causes reduction in AB interaction. Similar result have been reported by Guillaud, Crevaux [73] and Smit [74] in Mn-Zn, Co-Zn and Ni-Zn ferrites. The composition with x=1.00 does not show transition temperature at and above room temperature. Similar behavior of this composition was already observed from our dc resistivity and magnetization study. (Please see chap. IV and chap. V, Sec. A). Curie temperature values calculated from Upadhayay's model are also presnted in same table. It is observed that the Curie

temperature values obtained by Loria -Sinha technique are nearly same as those observed in dc resistivity and ac susceptibility studies.The values of Curie temperature observed in dc resistivity and ac susceptibility studies are also presented in table 5.2.

Table 5.2

Curie temperature data of Ni_{1-x} $Zn_xFe_2O_4$ system

Zinc content x	Curie temperature (Tc) from °C			
	Resistivity	**Susceptibility**	**Loria-Sinha**	**Upadhyay's model**
0.0	574	597	568	597
0.20	478	492	477	536
0.40	376	387	367	449
0.60	276	269	278	333
0.80	119	89	45	185
1.00		-	-	-

Part C : Susceptibility

5.C.1 Experimental

AC susceptibility measurement of powdered samples of $Ni_{1-x}Zn_xFe_2O_4$ (x=0, 0.20, 0.40, 0.60, 0.80 and 1.00) system were carried out in the

emperature range of 300 to 850K by using double coil set up operating at a frequency of 263 Hz in r.m.s field of 550 A/m [75].

The schematic diagram of ac susceptibility measurement system is shown in Figure 5.11.

The set up consist of double balancing coil having large number of turns acting as flux detector and was placed in between the Helmoltz coils. The furnace is fabricated by winding of platinum wire on a silica tube surrounded by a glass jacket placed at the center of the pick up coil. A cold water was circulated through the glass jacket inorder to prevent the pick up coil from overheating. A sample holder containing the sample under investigation was introduced in the furnace. The current to the Helmoltz coil was supplied from a oscillator and high quality power amplifier, which induces signal in the double coil. The signal induced in the double coil is proportional to the rate of change of magnetic moment of the sample. Then signal was amplified, rectified and read out on a digital voltmeter which was calibrated interms of magnetic moment.

The temperature of the furnace was raised by increasing current in the heating coil and was recorded by using a well calibrated platinum - rhodium thermocouple. The sample was heated gradually and at various temperatures signal was recorded. The heating of the sample was continued till the signal is reduced to zero.

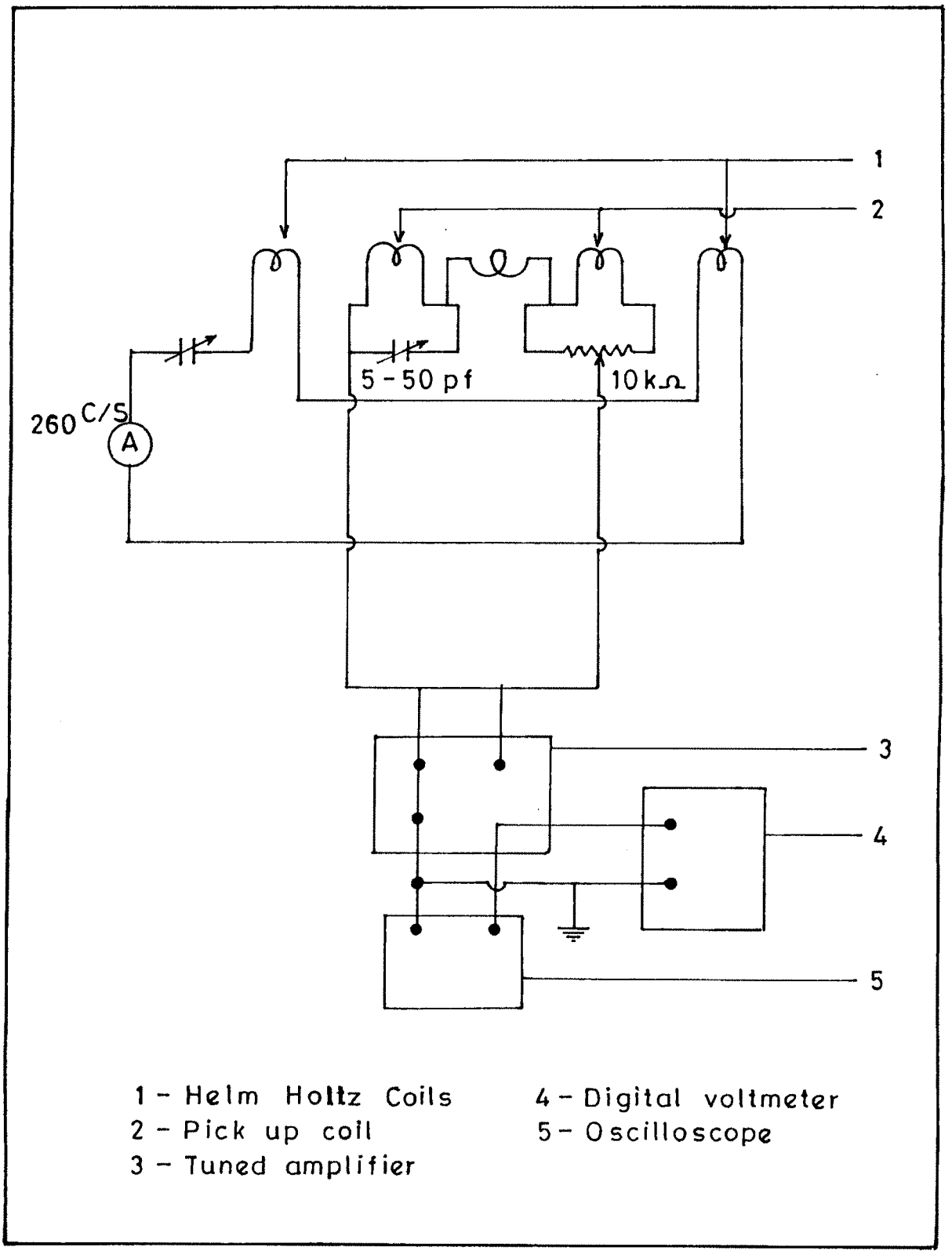

FIG. 5·11 - SCEMATIC DIAGRAM OF A.C. SUSCEPTIBILITY MEASUREMENT SYSTEM.

5.C.2 Results and discussion

The variation of normalized a.c. susceptibility (χ_T/χ_{RT}) as a function of temperature for the series $Ni_{1-x}Zn_xFe_2O_4$ with x=0.0, 0.20, 0.40, 0.60 and 0.80 is shown in figure 5.12.

From this figure it can be concluded that

1. The sample with composition x=0 and x=0.20 exhibit a peak at higher temperature and then drop sharply near Curie temperature (T_c). The peaking behavior suggest that these compositions predominately contain single domain (SD) particles.

2. The sample with composition $x \geq 0.40$ does not show appreciable variation of normalized ac susceptibility with temperature. This suggests that multidomain (MD) particles are favoured within these sample.

3. All the samples show a sharp decrease in normalized a c susceptibility (χ_T/χ_{RT}) with temperature near Curie point, indicating impurity phases are not present in the samples which is already confirmed from XRD studies.

4. The peak height before Curie temperature is more pronounced for the composition x=0 than x=0.20 and completely disappears for the compositions $x \geq 0.40$, suggesting that addition of zinc forces the sample to go from SD to MD state [58].

Bulk magnetic studies on Cu-Zn ferrites is carried out by Sawant et al [39]. They have reported that, the peaks in χ_T/χ_{RT} variation with temperature decrease gradually on addition of zinc and disappear completely when

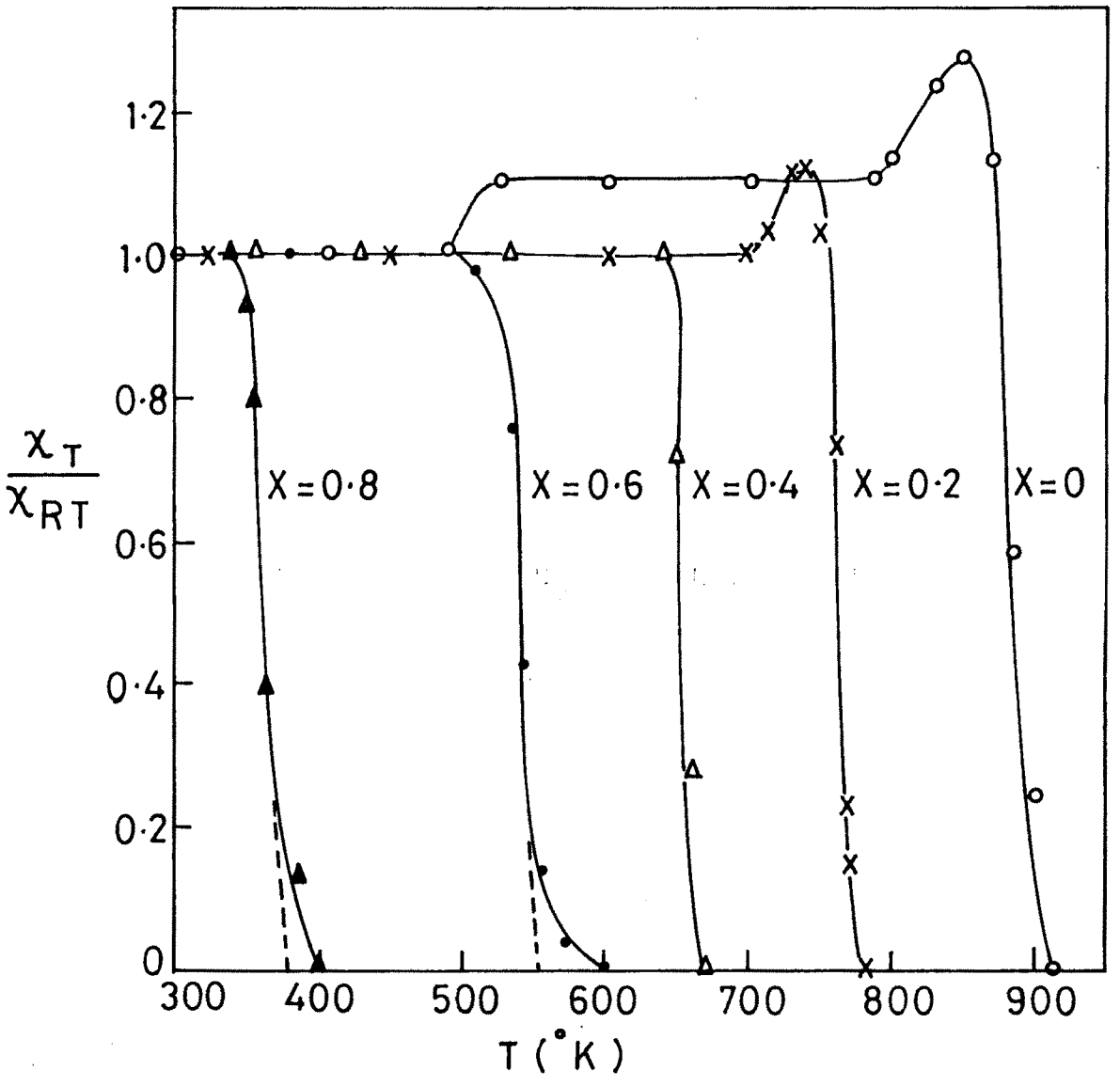

FIG. 5-12 - VARIATION OF NORMALIZED A.C. SUSCEPTIBILITY AS A FUNCTION OF TEMPERATURE FOR $Ni_{1-x}Zn_xFe_2O_4$ SYSTEM.

concentration of zinc is 0.6. The peak observed in χ_{ac}-T variation is attributed to SD-SP transition and addition of zinc forces the sample to go from SD to SD-MD state. Suryawanshi et al [45] carried out XRD and magnetic studies on Ti substituted Mg-Zn ferrites. They have shown that peaks observed in χ_T/χ_{RT} variation at blocking temperature becomes less pronounced on addition of zinc and disappear when zinc is added in excess of 20 %. The peaks in the χ_T/χ_{RT} variation with temperature was due to SD-SP transition and vanishing of this peaks suggest that the particles are SD.

References

1. Lax B and Button K.J, "Microwave ferrite and ferromagnetics", Mc.Graw Hill Book company, NY (1962).
2. Satya Murthy N.S., Natera M.G, Youssef S.I, Begum R.J and Srivastava C.M., Phys. Rev. 181 (1969) 969.
3. Srivastava C.M. and Patni M.j., J. Magn. Res. 15 (1974) 389.
4. Puri R.K., Reshmi Mitra and Kulkarni R.G., Proc. ICF - 5 (1989) 353.
5. Das A.R., Ananthan and Khan D.C., J. Appl. Phys. 57 (1) (1985) 4189.
6. Ghatage A.K. , Patil S.A. and Paranjape S.K., Indian J. Phys., 73 A (3) (1999) 329.
7. Pandya H.N and Kulkarni R.G., Solid state communications, 6 (10) (1987) 645.
8. Ghatage A.K, Choudhari S.C and Patil S.A., Journal of materials science lettres, 15 (1996) 1548.
9. Becker R and Kersten M., Z.Phys. 64 (1930) 64.
10. Lee E.W., "Magnetostriction and mangetochemical effect", Rept. Progr. Phys., 18 (1955) 184.
11. Briss R.R., "The saturation magnetization of ferromagnetics", Advan. Phys., 8 (1959) 252.
12. Murthy S.R. and Rao T.S., Phys. Stat Sol^{n}. (a) 90 (1985) 631.
13. Weiss D., J. de Physique, 6 (1907) 661.
14. Snoek A. L, Physica, 14 (1948) 207.

15. Polder D and Smith J., Rev. Syst. Phys., 25 (1953) 89.

16. Galt J.K., Bell. Syst. Tech. J. , 33 (1954) 1023.

17. Rao V and Keer H.V, Paramana, 19 (1982) 103.

18. Brailsford F., Physical Principle of magnetism (London Van Nostrand) (1966) 166.

19. Keer H.V., "Principle of the solid state", Wiley Eastern limited", (1993) 238.

20. Chaugule R.S., Radhakrishnamurthy C., Sampathkumaran E.V., Malik S.K. and Vijayaraghavan R., Mat. Res. Bull. Vol. 18 (1983) 817.

21. Neel L., Adv. Phys., 4 (1955) 191.

22. Radhakrinshnamurthy C., Likhite S.D., Deutsch E.R.and Murthy G.S., Phys. Earth Planet. Inter., 30 (1982) 30.

23. Bean C.P., J. of Applied Physics, 26(1) (1955) 1381.

24. Radhakrishnamurthy and Nanadikar N.G., paramana, 3 (4) (1979) 413.

25. Galt J.K., Matthias B.J., and Remeika J.P., Ibid, 79 (1950) 391.

26. Healy D. W., Phys. Rev., 86 (1952) 1009.

27. Bozorth R.M, Tilden E.F. and williams A.J., Phys. Rev. 99 (1955) 178.

28. Yager W.A., Galt J.K and Merrit F.R., Phys. Rev., 99 (1955) 1203.

29. Oillon J.F, Geschand S amd Jaccarino V., ibid, 100 (1955) 750.

30. Bickford L.R., Phys. Rev., 78 (1950) 449.

31. Bozorth R.M., Cetin B.B., Galt J.K, Merritt F.R. and Yager W.A., ibid, (1955) 1898.

32. Bickford L.R. Brownlow J.M. and Penoyer R.F, Proc. IEE B, 104 (15) (1957) 238.

33. Kakatkar S., Chaudhari N, Sankapal A., Patil R. Sawant S.R. and Patil, R.N., J. of Physics, 21 (1997) 677.

34. Gorter E. W. Philips Res. Rept., 9 (1954) 321.

35. Neel L., Ann. Phys. 3 (1948) 137.

36. Gilleo M.A., J. Phys and Chem.Solids, (GB) 13 (1960) 33.

37. Upadhyay R.V., Indain J. Phys., 63A (8) (1989) 835.

38. Valenzuela., J. Mater. Sci. (GB) 15 (12) (1980) 3175.

39. Sawant S.R., Birajdar D.S, Suryavanshi S.S., Sankapal A.M., Patil, B.L, Patil, S.A., and Patil R.N., Indian J. of Pure and Appl. Phys., 28 (1990) 4241.

40. Niak A.B. and Powar J.I., Indian J. of Pure and Appl. Phys., 23 (1985) 436.

41. Bhise B.V., Mahajan V.C., Patil M.G., Lotke S.D. and Patil S.A., Indian J of Pure and Appl. phys., 33 (1995) 459.

42. Bhise B.V., Patil M.G., Dongare M.B., Sawant S.R and Patil S.A., Indian J. of Pure and Appl. phys., 30 (1992) 385.

43. Baijal J.S., Kothari D., and Phanjoubam S., Proc. ICF - 5 (1989) 371.

44. Karche B.R., Khasbardar B.V. Vaingankar A.S., J. of Magnetism and Magneic Materials, 168 (1997) 292.

45. Suryavanshi S.S., S.A. Patil, Jadhav C.N. and Sawant S.R., Mat. Res. Bull. 24 (1989) 1201.

46. Kolekar C.B., Kamble P.N. and Vaingankar A.S., Indian J. Phys., 68 A (6) (1994) 529.

47. Bhosale J.L, Kulkarni S.N, Sasmile R.B and Chougule B.K,Bull. Mater. Sci., 19 (5) (1996) 767.

48. Ghatage A.K, Patil S.A., and Paranjape S.K., Indian. J. of Phys., 72 A (3) (1998) 209.

49. Patil S.H., Patil S.I., Kadam S.M. and Chougule B.K, Indian Journal of Pure and Appl. Physics, 30 (1992) 183.

50. Pasnicu C., Condurache D., Luca E., Phys. Status Solidi (a) 76 (1) (1983) 145.

51. Bhosale J.L, Kulkarni S.N., Sasmile R.B. and Chougule B.K, Bull . Mat. Sci., 19 (5) (1996) 767.

52. Bellad S.S and Chougule B.K, Mater. Research Bulletin, 33 (8) (1998) 1165.

53. Bhosale D.N., Chaudhari N.D., Sawant S.R. and Kale R.D., IEEE Trans. on Magnetics., 34 (2) (1998) 536.

54. Bhosale D.N., Chaudhari N.D., Sawant S.R. and Bakare P.P.., J. of Magetisum and Magnetic Materials, 173 (1997) 51.

55. Vasambkear P.N, Kolekar C.B, and Vaingankar A.S., J. of Magnetisum and Magnetic Materials, 186 (1998) 333.

56. Kolekar C.B., Ladagonakr B.P, Vasamberkar P.N and Vaingankar A.S., DAE solid state symposium, Indira Gnadhi Centre for Atomic Research, Kalapakkam- Tamlinadu (1999).

57. Radhakrishnmurthy C., Likhite S.D and Satry N.P., Phil. Mag., 23 (1971) 503.

58. Shinde T.J., Ladgaonkar B.P., vasamberkar P.N. and Vaingankar A.S., National conference on recent trends in matreial science (Tirupati) (1999).

59. Daniels J.M and Rosenwaig A., Can. J. of Phys., 4, (48) (1970) 381.

60. Smit J. and Wijn H.P.J., "Phsyical properties of ferrimagnetic oxides in relation to their technical applications" Phlips Tech. Lab. (1959) 151.

61. Satya Murthy N.S., Natraj M.G., Youssef S.I and Begum R.J., Physical review, 2 (181) (1969) 969.

62. Guillaud C., ibid (1950) 1458.

63. Guillaud C and Roux M., C.R. Acad. Sci. Paris., 229 (1949) 1133.

64. Gorter E.W., Philips Research Repts., 165 (1954) 321.

65. Lenug L.K., Evans B.J. and Morrish A.H., Phys. Rev. B. 8 (1973) 29.

66. Srivastava C.M., Shringi S.N., Srivastava R.G. and Nandikar N.G., Physical Review, B 14 (5) (1976) 2032.

67. Joshi G.K, Khot A.Y and Sawant S.R, Solid State Commun., 65 (12) (1988) 1593.

68. Smit J. Wijn H.P.J, "Ferrites, philips Technical Library Eindhaven, the Netherlands", (1959) 158.

69. Verma A., Goel T.C., Mendiratta R.G. and Gupta R.G., J. of Mag. and Magnetic materials, 192 (1999) 271.

70. Puri R.K., Babbar V.K. and Mendiratta R.G., Proc. ICF- 5 (1989) 239.

71. Bhosale D.N, Choudhari N. D, Sawant S.R., Kale R and Bakare P., IEEE Trans. on Magnetics, 34 (2) (1998) 535.

72. Loria K.K. and Sinha P.B., Ind. Acad. Sci., (Earth Planet Sci) 87 (1978) 245.

73. Guillaud C and Crevaux H., C.R. Hebed Seans Sci. Paris, (1950) 229.

74. Smit J., Mag. Props. of Materials, MGH co. NY, (1971) 216.

75. Radhakrishnamurthy C., Likhite S.D., and Sahastrabudhe P.N., Proc. Ind. Acad. Sci. (Earth Planet Sci) 87 (1978) 245.